

# HIGH GAIN ADVANCED GPS RECEIVER

Dr. Alison Brown, Gengsheng Zhang; NAVSYS Corporation

## ABSTRACT

NAVSYS High Gain Advanced GPS Receiver (HAGR) uses a digital beam-steering antenna array to enable up to eight GPS satellites to be tracked, each with up to 10 dBi of additional antenna gain over a conventional receiver solution. This digital, PC-based architecture provides a cost-effective solution for commercial applications where more precise GPS measurements are needed.

The additional gain provided on the satellite signals by the HAGR enables sub-meter Pseudo-ranges to be observed directly on the C/A code and also improves the accuracy of the GPS carrier phase and estimates of the satellite signal strength. The directivity of the digital beams created from the antenna array also reduces multipath errors further improving the accuracy of DGPS corrections generated by the HAGR and the navigation and timing solution computed.

This paper describes the beam steering array and digital receiver architecture and includes test data showing the HAGR performance.

## HIGH GAIN ADVANCED GPS RECEIVER DESIGN

The HAGR design is based on NAVSYS' Advanced GPS Receiver (AGR) PC-based digital receiver architecture<sup>1</sup> integrated with a digital beam steering array. Using a proprietary digital signal processing algorithm NAVSYS is able to combine data from as many as 16 antennas and create a multi-beam antenna pattern to apply gain to up to eight GPS satellites simultaneously. In Table 1, the performance specifications for NAVSYS beam steering array and AGR receiver are shown for different antenna array configurations. The AGR receiver specification is shown in Table 2.

**Table 1 Digital Antenna Array Gain**

#Antenna Elements	Ideal	Spec
2	3 dB	2 dB
4	6 dB	5 dB
9	9 dB	7 dB
16	12 dB	10 dB

**Table 2 AGR Performance Specifications**

Technical Specifications	
GPS Frequency	L1, 1575.42 MHz
Source	C/A code (SPS)
Channels	8 channels
Correlation	Adjustable Spacing
Operating Specifications	
Signal Acquisition	32 dB-Hz (single element)
Signal Tracking	34 dB-Hz (single element) 24 dB-Hz (16 element array)
Time To First Fix	40 secs (cold – no time or position)
Re-Acquisition	10 secs to valid position
DFE Input Signals	
Center Frequency	1227.6 to 1575.42 MHz
Nominal Signal Level	-136 to -86 dBm
Signal Bandwidth	0 to 20 MHz
CW or Noise Interference Levels at DFE Input	
Center Frequency $\pm$ 10 MHz	10 dB above weakest
1200 to 1600 MHz	<-80 dBm
Outband Interference	<-20 dBm
Built-in Modules	DGPS (reference and remote) Timing Reference Beam steering
DFE Output Signals	
Digital Samples	I, Q, or I&Q
A/D	1-4 bits
Sample Rate	2-25 MHz
IF Frequency	70 MHz
User Configuration Parameters	Vehicle Dynamics
Selectable through configuration file or user interface	Track Thresholds DLL and PLL or FLL bandwidths and thresholds DFE characteristics Correlator spacing Data logging rates Satellite selection methods

The HAGR system is shown in Figure 1 and consists of the components shown in Figure 2. A multi-element antenna array is assembled using commercial antenna elements. The antenna outputs are fed to a Digital Front End (DFE) assembly which includes a custom RF-board that digitizes each of the received L1 signals. The digital output from the DFE assembly is then passed to a custom Digital Beam Steering (DBS) board installed in the AGR Personal Computer that performs the digital signal

processing required to implement the digital beam steering operations. The AGR PC also includes a custom Correlator Accelerator card (CAC) that performs the C/A code correlation and carrier mixing on each satellite channel.



Figure 1 HAGR System

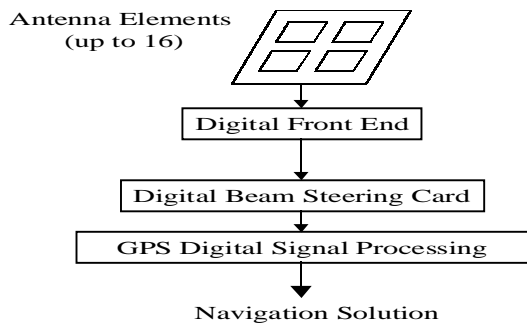


Figure 2 High Gain Advanced GPS Receiver Design

Depending on the level of performance desired, the antenna array and DFE assembly can be populated with two, four, nine or sixteen antenna elements. The antenna array configurations are shown in Figure 3. The antenna elements are spaced 1/2 wavelength apart.

The Digital Beam Steering board is operated through software control from the AGR PC. This applies the array DSP algorithms to form the digital antenna array pattern from the multiple antenna inputs, adjusts the antenna array pattern to track the satellites as they move across the sky, and applies calibration corrections to adjust for offsets between the individual antenna and DFE channels and alignment errors in the positioning of the antenna elements and array assembly.

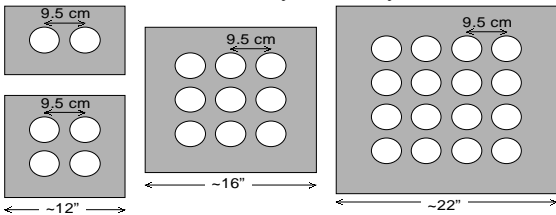


Figure 3 Alternative Antenna Array Configurations

The GPS signal processing is performed by the HAGR Correlator Accelerator Card (CAC) also operated under

software control from the PC. This performs the code and carrier tracking on each satellite signal. The HAGR PC-based software computes the navigation solution using the satellite data and can also be configured to record raw measurement data or generate differential GPS (DGPS) or kinematic GPS (KGPS) corrections.

ANTENNA ARRAY BEAM PATTERNS

The beam pattern created by the digital antenna array is a function of the number of elements used in the array and the elevation angle of each satellite being tracked. In Figure 4, simulated beam patterns are shown for the different HAGR antenna configurations. In Figure 5 a typical beam pattern to a single GPS satellite is shown for a 16-element array.

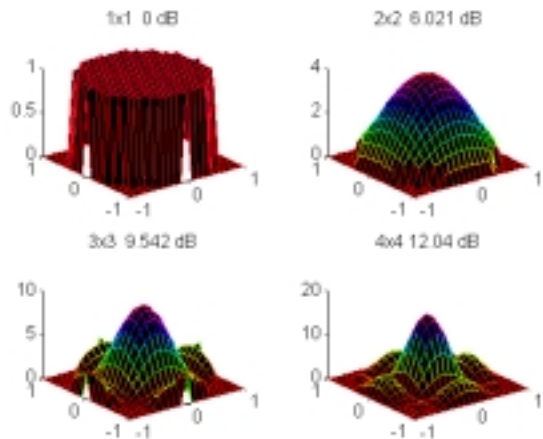


Figure 4 Typical antenna beam patterns

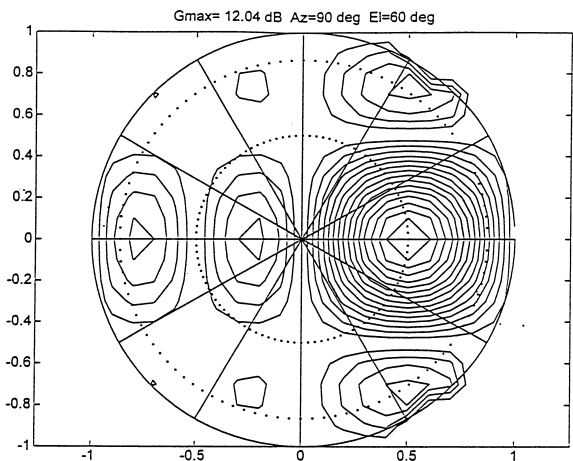
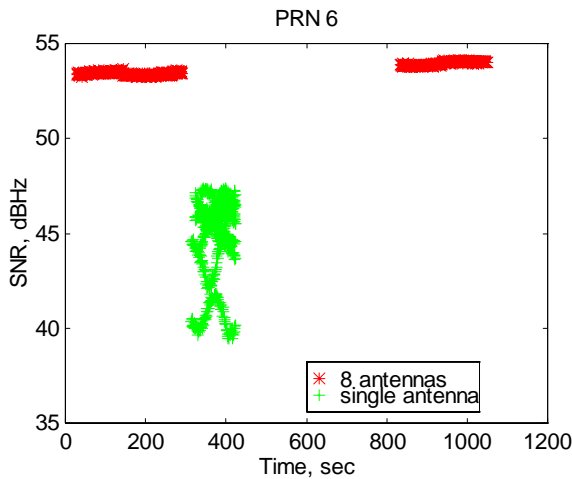


Figure 5 Single Satellite 16-element Digital Array Beam Pattern

## HAGR SIGNAL-TO-NOISE RATIO COMPARISON TESTING

The improved gain possible using the HAGR was demonstrated by collecting test data using the HAGR in an 8-antenna configuration. First the C/No was collected from the digital beam-steered data, then the C/No data was collected tracking each antenna element on a different channel of the HAGR. This data is illustrated in Figures 6 through 9.



**Figure 6 Signal Noise Ratio Comparison between Single Antenna and 8 Antennas for PRN**

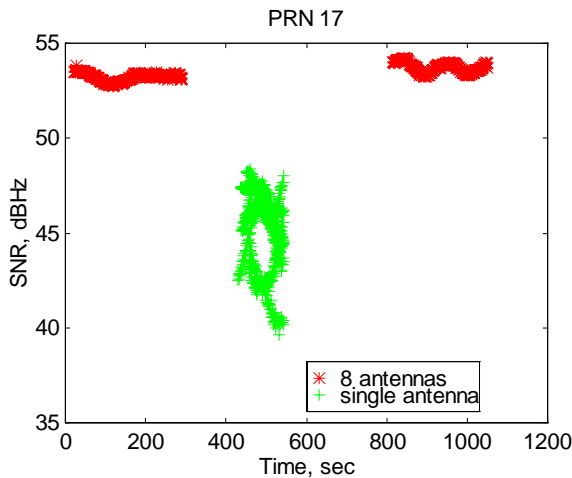


**Figure 7 SNR Comparison between Single Antenna and 8 Antennas for PRN 17**

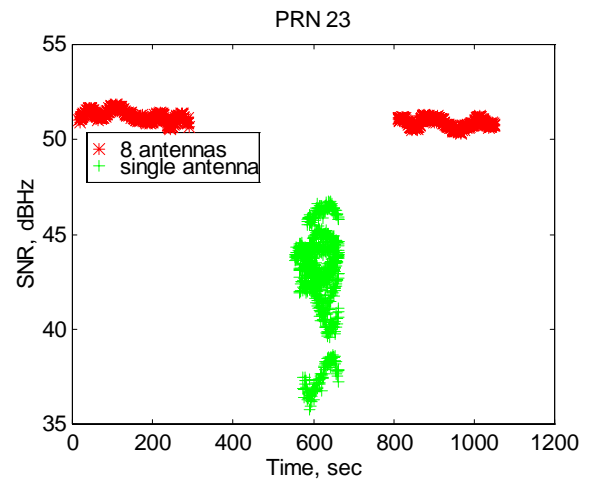


**Figure 8 SNR Comparison between Single Antenna and 8 Antennas for PRN 23**

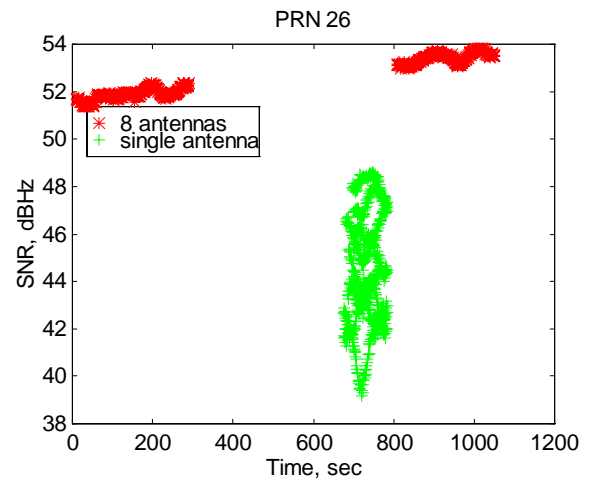


**Figure 9 SNR Comparison between Single Antenna and 8 Antennas for PRN 26**

The C/No on the individual elements varies over time due to multipath constructive/destructive interference on the received signals. The combined C/No generated from the digital beam does not show this variation, demonstrating that the multipath errors have been significantly reduced, and the over-all C/No is increased to 51 to 54 dB-Hz.

In Figures 10 through 16 the HAGR C/No is shown compared against the C/No observed by a conventional GPS receiver. This shows that with the 8-element antenna array, gains of between 6 to 8 dB were observed. These Figures also illustrate that the noise on the C/No estimate from the HAGR data is much less than the noise from the conventional GPS receiver C/No.

## HAGR PSEUDO-RANGE NOISE

The HAGR pseudo-range measurement accuracy was demonstrated by plotting the difference between the pseudo-range and the contiguous carrier phase observations. This difference is a function of the pseudo-range measurement noise, the carrier-phase noise ( a minimal effect) and the code/carrier divergence caused by the ionosphere (which is constant over short time intervals). This data is plotted in Figures 17 through 22 and shows that the pseudo-range variance is between 0.6 to 1 meter for the unfiltered HAGR data. It should be noted that with carrier smoothing, this variance would be reduced even further. The observed pseudo-range noise compares closely with that predicted by the improved C/No. For example, at a C/No of 54 dB-Hz, theory predicts a pseudo-range variance of 0.4 meters. Our data shows an observed variance of 0.5 meters for the same C/No.

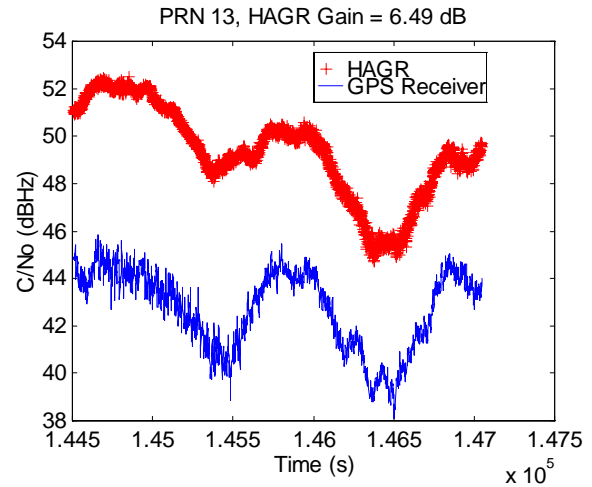


**Figure 12 SNR Comparison between 8-Antenna HAGR and Conventional Receiver**

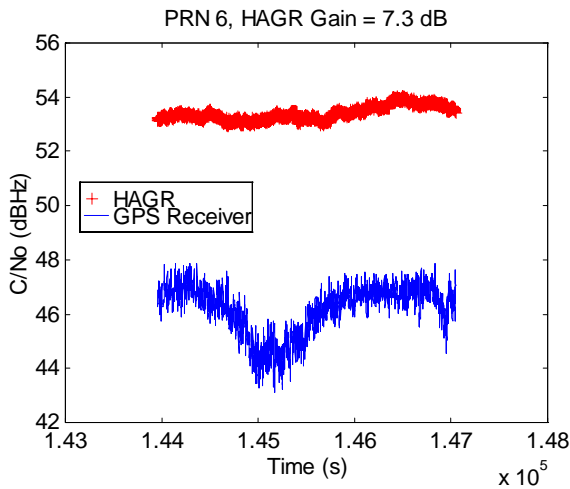


**Figure 10 SNR Comparison between 8-Antenna HAGR and Conventional Receiver for PRN 6**

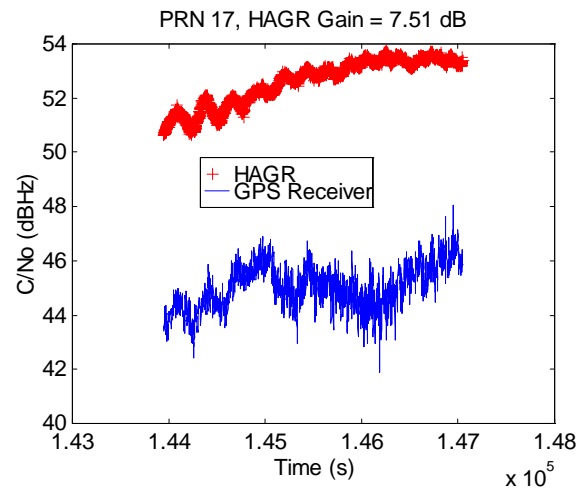


**Figure 13 SNR Comparison between 8-Antenna HAGR and Conventional Receiver**

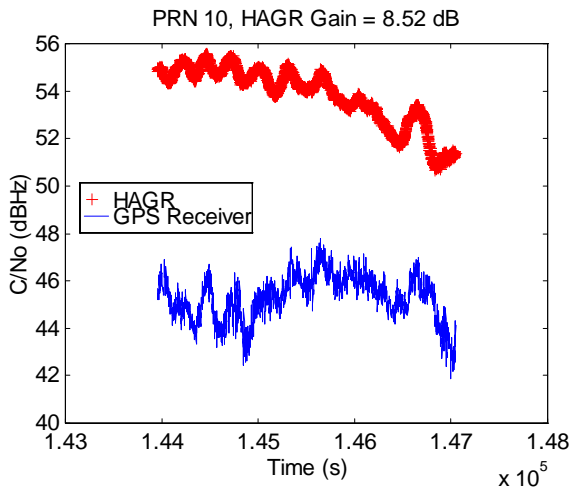


**Figure 11 SNR Comparison between 8-Antenna HAGR and Conventional Receiver for PRN 13**

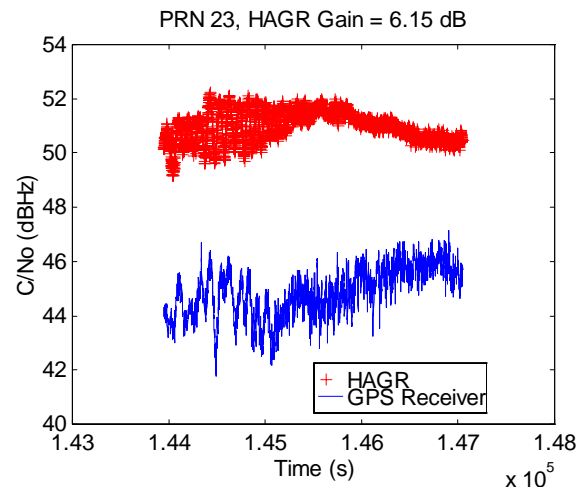


**Figure 14 SNR Comparison between 8-Antenna HAGR and Conventional Receiver**

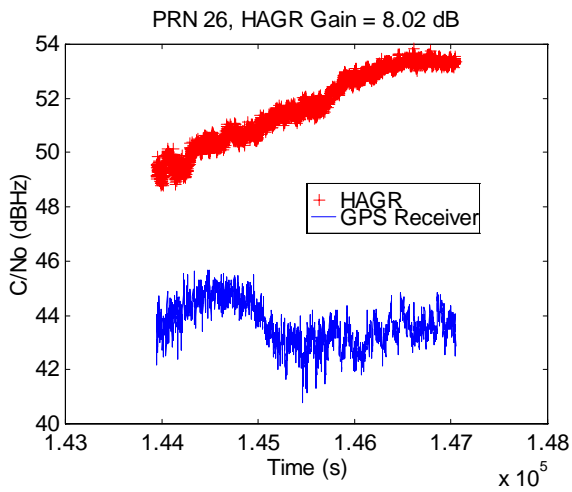


**Figure 15 SNR Comparison between 8-Antenna HAGR and Conventional Receiver**

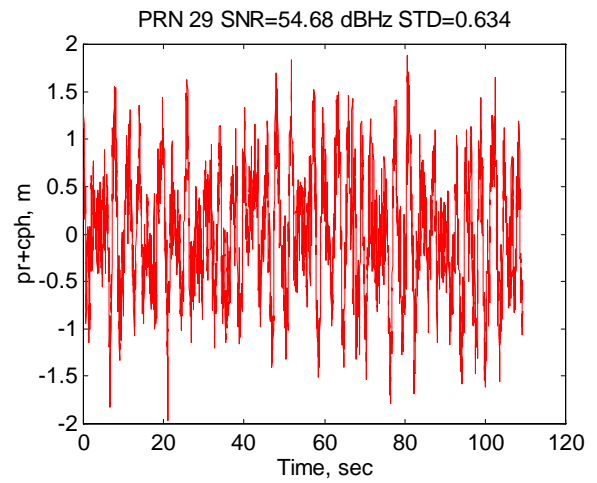


**Figure 18 HAGR Difference between Pseudo-Range and Carrier Phase for PRN 29**

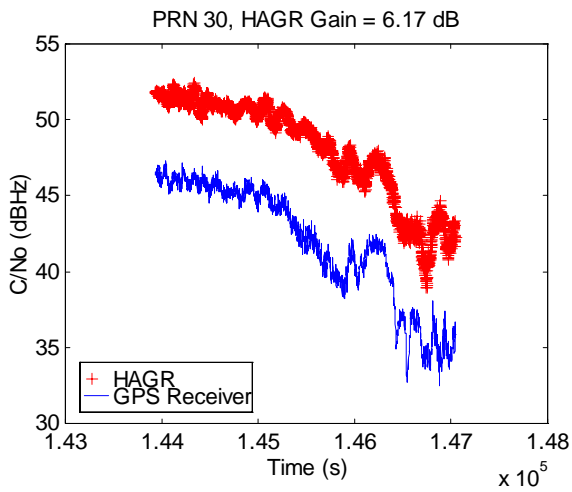


**Figure 16 SNR Comparison between 8-Antenna HAGR and Conventional Receiver**

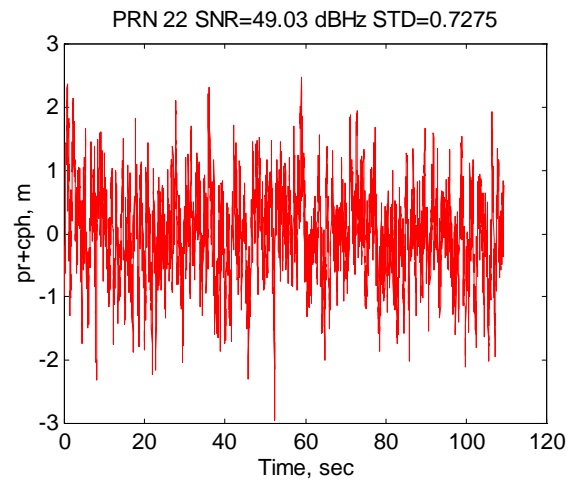


**Figure 19 HAGR Difference between Pseudo-Range and Carrier Phase for PRN 22**

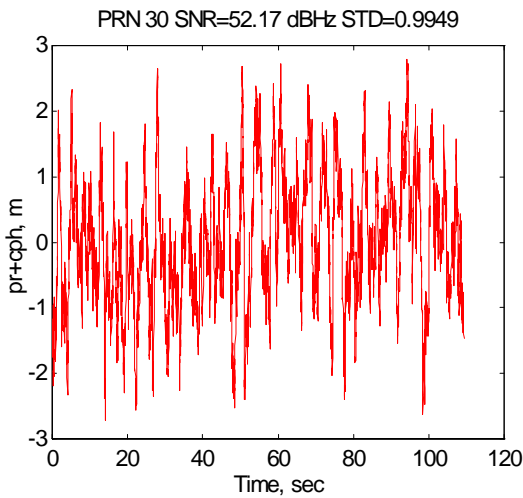


**Figure 17 HAGR Difference between Pseudo-Range and Carrier Phase for PRN 30**

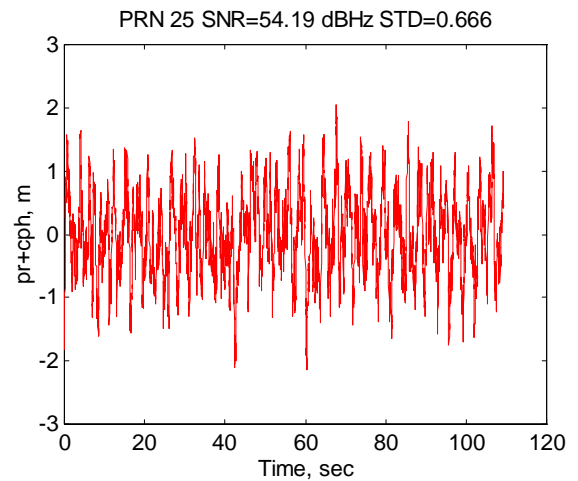


**Figure 20 HAGR Difference between Pseudo-Range and Carrier Phase for PRN 25**

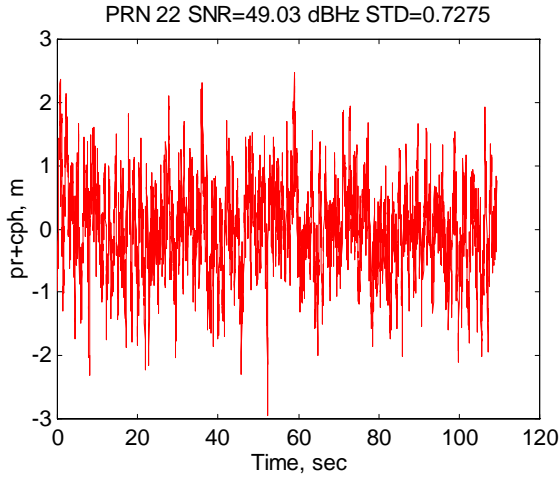


**Figure 21 HAGR Difference between Pseudo-Range and Carrier Phase for PRN 22**

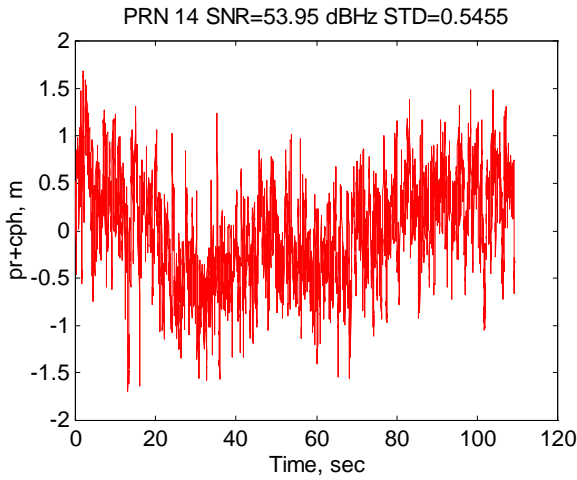


**Figure 22 HAGR Difference between Pseudo-Range and Carrier Phase for PRN 14**

### HAGR CARRIER PHASE OBSERVATIONS

The HAGR beam steering equations are tuned to steer the observed carrier phase from each element to the center of the array. To test the carrier phase observation accuracy, two reference antennas each connected to a reference GPS receiver were located equally spaced on either side of the array. The carrier phase observations from these reference receivers were average to estimate the phase observed at the center of the array and then double-differenced with the HAGR carrier phase outputs. This residual observes the following errors.

$$z_{\phi} = \phi_i^{HAGR} - \phi_2^{HAGR} - 0.5(\phi_i^A + \phi_2^B) + 0.5(\phi_2^A + \phi_2^B)$$

$$\sigma_z = \sqrt{2}(\sigma^{HAGR} + \sigma^{RX})$$

The residual error is plotted in Figures 23 through 27 showing that the HAGR phase center agrees with the predicted antenna array phase center. The residual

standard deviation is dominated by the noise from the reference receivers but is within 0.02 cycles (4 mm) on each case.

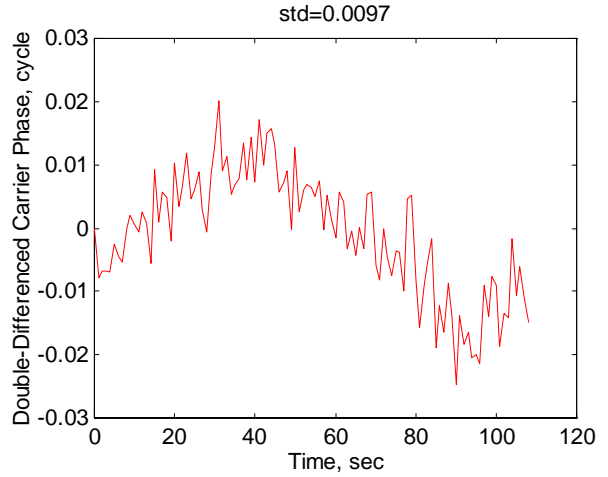


**Figure 23 Double-Differenced Carrier Phase between PRN 30 and PRN 29**

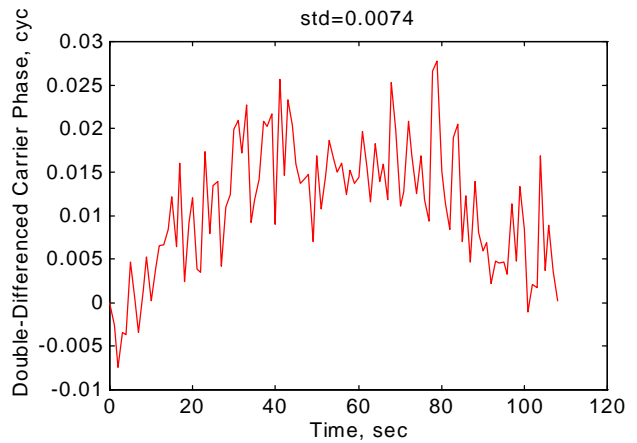


**Figure 24 Double-Differenced Carrier Phase between PRN 30 and PRN 25**

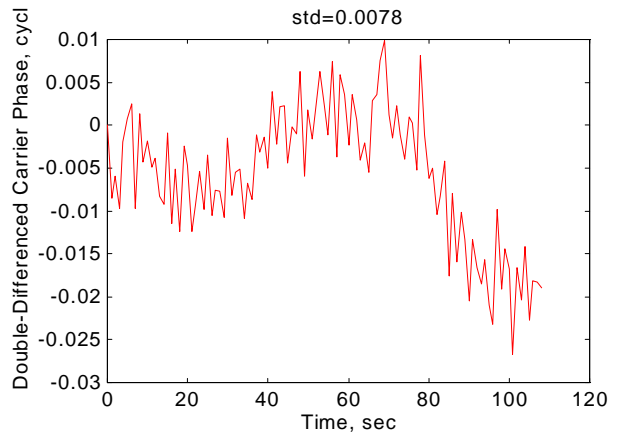


**Figure 25 Double Differenced Carrier Phase between PRN 30 and PRN 22**

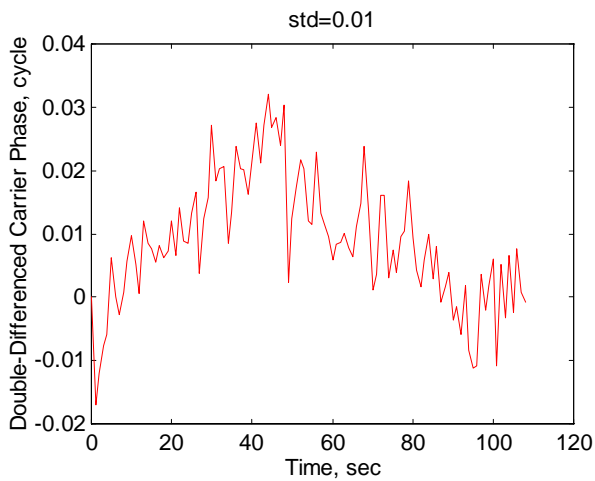


**Figure 26 Double Differenced Carrier Phase between PRN 30 and PRN 15**

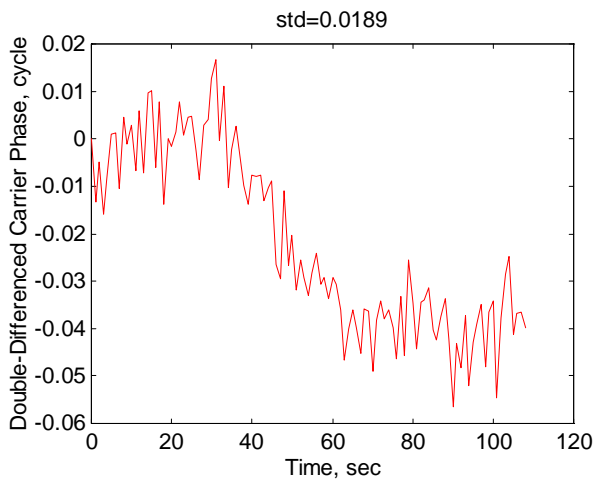


**Figure 27 Double-Differenced Carrier Phase between PRN 30 and PRN 14**

The short term HAGR carrier phase noise can best be observed using single-differenced satellite measurements and removing the satellite and clock effect. The short-term noise from HAGR carrier phase data collected at a 50 Hz rate is plotted in Figures 28 through 32. This shows that the HAGR carrier phase standard deviation from short term noise is within 0.6 mm ( $0.005/\sqrt{2}$  cycles) on each channel.

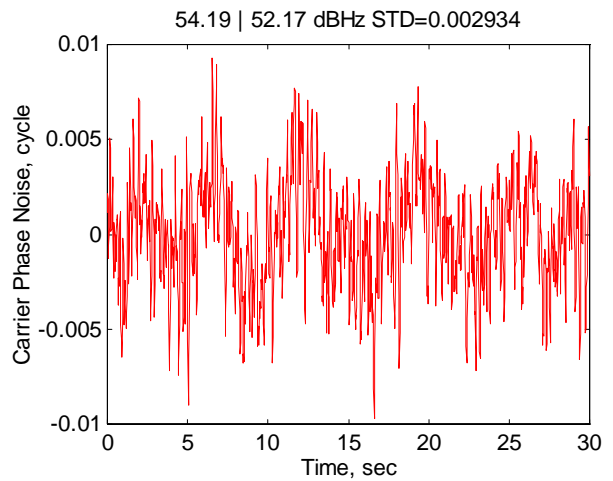


**Figure 28 Single Difference HAGR Carrier Phase Noise between PRN 30 and PRN 29**

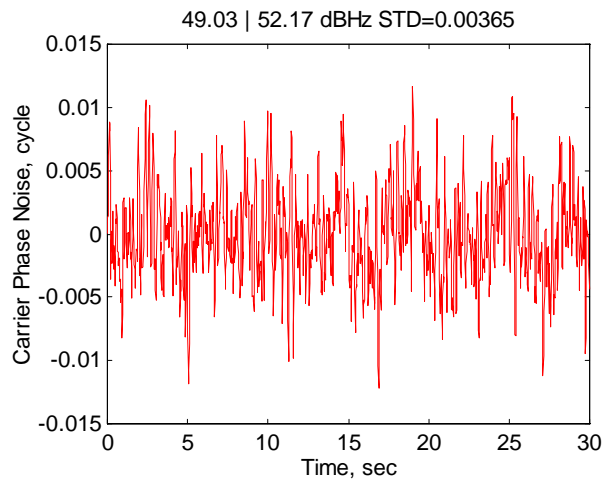


**Figure 29 Single Differenced HAGR Carrier Phase Noise between PRN 30 and PRN 25**

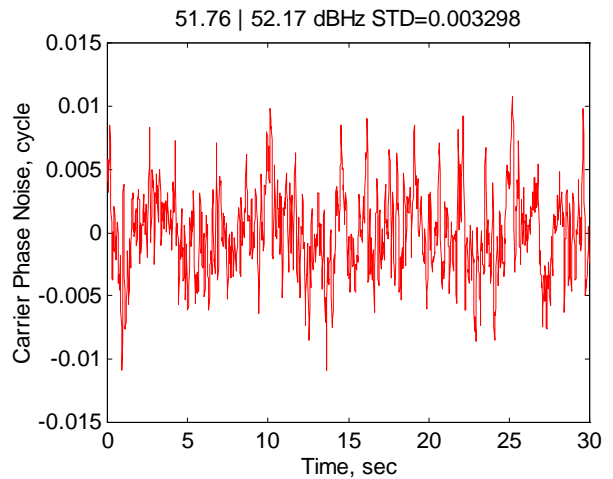


**Figure 30 Single Differenced HAGR Carrier Phase Noise between PRN 30 and PRN 15**

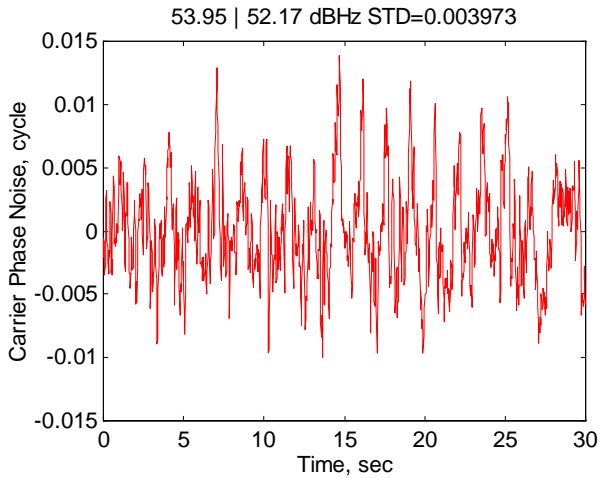


**Figure 31 Single-Differenced HAGR Carrier Phase Noise between PRN 30 and PRN 14**

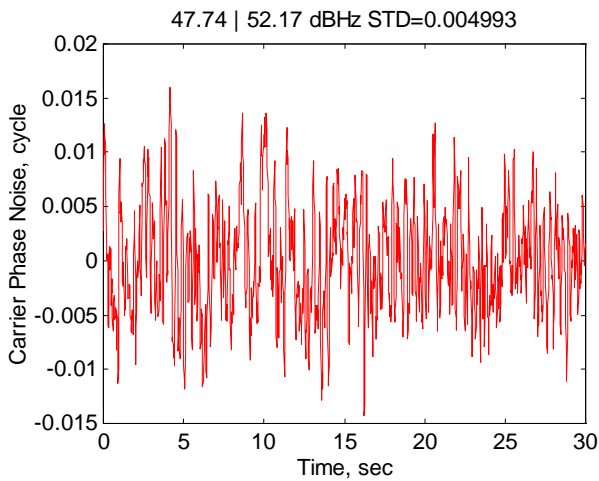


**Figure 32 Single-Differenced HAGR Carrier Phase Noise between PRN 30 and PRN 1**

## CONCLUSION

In this paper, the design, performance and test results of the NAVSYS High Gain Advanced GPS Receiver (HAGR) have been presented. The benefits of the HAGR for the following applications are summarized below.

### Differential Reference Station

The gain applied to the GPS signals by the antenna array improves the signal strength observed in the tracking loops by up to 10 dBi (for the 16-element array option). This will improve the pseudo-range residual noise from the AGR's delay lock loops by a factor of 3. The improved pseudo-range accuracy results in higher precision in differential corrections generated by this reference receiver. The variance on unfiltered 1-Hz pseudo ranges collected into the HAGR was shown to be between 0.5 and 1 meters.

### Multipath Rejection

The antenna array digital signal processing algorithms applied by the programmable Digital Beam Steering (DBS) PC-board can be optimized to reject satellite signals received at low elevations. This attenuates any multipath signals received while applying gain to the direct path GPS satellite signals. The combination of these effects is to significantly reduce the residual multipath error in the AGR's delay lock loops and pseudo-range and comer phase observations.

### Interference Rejection

The antenna array digital signal processing algorithms applied by the programmable DBS-board can be programmed to apply nulls as well as generate gain through forming beams. By placing nulls on interfering signals, the DBS-board can also be used to reject interference sources or signals from GPS jammers.

### Ionospheric Monitoring

The high gain antenna array enables the NAVSYS receiver to track GPS signals down to 22 dB-Hz signal-to-noise ratio. This enables the NAVSYS reference receiver to continue to provide ionospheric test data from GPS satellites through scintillation signal fades in excess of 20 dB<sup>2</sup>.

## ACKNOWLEDGEMENT

Much of this work was sponsored under the Air Force SBIR contract F19628-97-C-0029, "High Gain Portable GPS Antenna Array for Ionospheric Monitoring."

## REFERENCES

- <sup>1</sup>,E. Holm, A. Brown, R. Slosky "A Modular Reprogrammable Digital Receiver Architecture," ION 54<sup>th</sup> Annual Meeting, Denver, CO, June 1998
- <sup>2</sup> A.Brown, E. Holm, K. Groves, "GPS Ionospheric Scintillation Measurements using a Beam Steering Antenna Array for Improved Signal/Noise", ION 54<sup>th</sup> Annual Meeting, Denver, CO, June 1998